Journal of Computer-Aided Molecular Design, **14:** 369–382, 2000.
KLUWER/ESCOM

Conformational analysis of a farnesyltransferase peptide inhibitor, CVIM

Louis Carlacci
Department of Chemistry, CHE 305, University of South Florida, Tampa, FL 33620, U.S.A.; E-mail: lou@finch.cas.usf.edu

Received 3 June 1999; Accepted 22 November 1999

Key words: cluster analysis, conformational library, conformational search, conformers, ionization, Metropolis Monte Carlo, Monte Carlo simulated annealing, Ras, solvation, states

Summary

The conformational states of the peptide Cys-Val-Ile-Met (or CVIM) were computed and characterized. CVIM inhibits farnesylation of the Ras oncogene product, $p21^{ras}$, at the cysteine residue of the C-terminal segment. CVIM is active in an extended conformation. A similar peptide (KTKCVFM) appears to bind the enzyme in the Type I bend conformation. In the present study, the conformations of CVIM were computed in an aqueous environment with the peptide in the zwitterionic state. Solvation free energy based on solvent accessible surface area and a distance dependent dielectric were used in the calculations. Final conformations of multiple independent Monte Carlo simulated annealing (MCSA) conformational searches were used as starting points for Metropolis Monte Carlo (MMC) runs. Conformations saved at intervals during MMC runs were analyzed. Conformers were separated by interactive clustering in dihedral angle coordinates. The four lowest energy conformers corresponding to a Type I bend, extended, AB-bend, and BA-bend were within 0.3 kcal/mol of each other, and dominant in terms of population. The Type I bend and extended conformers were supported by the binding studies. The extended conformer was the most populated. In the AB-bend conformer, 'A' indicates the α-helix conformation of Val, and 'B' indicates the β-strand conformation of Ile. The AB- and BA-bend conformations differed from the extended conformation in the value of Val ψ and Ile ψ, respectively, and from the Type I bend conformation in the value of Ile ψ and Val ψ, respectively. The four lowest energy conformers were characterized in terms of energy, density of low energy conformations (or entropy), structure, side chain rotamer fraction population, and interatomic distances.

Introduction

In mammals, Ras is a 21 kDa guanine nucleotide binding protein that regulates the transduction of biological information from the plasma membrane to the nucleus [1]. Oncogenic mutations give rise to a protein that can bind but not hydrolyze GTP, which results in uncontrolled growth [2]. Ras association with the plasma membrane via a covalently linked lipid group is a necessary step in the signaling process [3]. Ras is post-translationally modified by the covalent attachment of a farnesyl group to the sulfur atom of the Cys residue of the C-terminal sequence CAAX (A = aliphatic, and X = methionine or serine) [4]. The enzyme called farnesyltransferase (or FTase) catalyzes this reaction [5]. Next, the AAX peptide is removed and the C-terminal carboxyl is methylated [6]. FTase is a metalloenzyme composed of an α subunit of 49 kDa and a β subunit of 46 kDa [7]. Inhibition of FTase provides a target for drug design since Ras is not able to associate with the plasma membrane without the attached lipid.

The Cys-Val-Ile-Met peptide (called CVIM) is the C-terminal segment of $p21^{ras}$. CVIM inhibits FTase in vitro by acting as an alternative substrate, but has no effect on whole cells [8]. Experimental studies of peptide mimetics and pseudopeptides that inhibit FTase activity have been reported (see Reference 9 for a list). Qian et al. demonstrated that the central dipeptide of the CA_1A_2X box is essential for farnesylation [10,11]. In the most potent inhibitor, A_1A_2 was substituted with an aromatic spacer that does not allow a turn conformation, and the distance between

atom Cys S^{γ} and the C-terminal carboxyl group in the pseudopeptide was close to the corresponding distance in the extended conformation of the peptide, about 10.5 Å. The hydrophobic property of A_1A_2 supports a complementary hydrophobic region in FTase. Leonard et al. [12] showed that a pentapeptide derivative that lacks cysteine inhibits FTase. In an NMR study on the binding of the KTKCVFM peptide to FTase, Stradley et al. [13] observed a Type I β-turn conformation of the CVFM segment. The results in References 11 and 13 suggest more than one binding conformation of the peptide.

The methodology used in the conformational analysis on Met^5-Enkephalin (Met-Enk), a five-residue peptide with sequence YGGFM [14], was used with some modifications in the present study. The final conformations of multiple independent Monte Carlo simulated annealing (MCSA) conformational searches were used as starting points for room temperature Metropolis Monte Carlo (MMC) trajectories that probe the potential energy surface. The peptide was computed in an aqueous environment given by the ionized peptide, a continuum solvation model, and a distance dependent dielectric of 2r. The low energy conformational states (or conformers) were several bend conformers and a significantly populated extended conformer. A low energy bend conformation satisfied the important pharmacophoric requirements of the morphine model of μ-receptor binding. Both the Met-Enk study and the present study analyzed conformations of the isolated peptide in various environments. Specific interactions between the peptides and their receptors were not considered.

Clustering algorithms were used to separate conformers and to analyze long molecular dynamics trajectories. The clustering algorithm that was developed and implemented in the Met-Enk study [14] was similar to the algorithm that was used by McKelvey et al. [15], which followed earlier ideas of Zimmerman et al. [16]. Peptide conformers were identified by assigning each residue to a region of the map of φ/ψ dihedral angles. (Dihedral angles were defined in accordance with the IUPAC-IUB Commission on Biochemical Nomenclature [17].) A single φ/ψ-map was used for all residues and for all conformers. In these studies, a clean separation of conformational states was not possible when a cluster of conformations lies in two different main chain rotamer regions (or φ/ψ pair or ω mc-rotamer regions), or when two conformational states lie in the same mc-rotamer region. Karpen et al. [18] analyzed conformations saved during long molecular dynamics trajectories by statistical clustering in n-dimensional dihedral angle space, which produced a set of dihedral angles for each cluster, followed by multidimensional scaling to project the clusters onto a two-dimensional plane. Clustering in dihedral angle space has the advantage over Cartesian space in that the clusters can be visualized in two-dimensional main chain and side chain dihedral angle scatter plots. In this study, each conformer was interactively separated by specifying the φ/ψ pair, and ω, rotamer regions that select the clusters of dihedral angle conformations. The χ rotamer regions were not interactively specified.

A conformer is defined as a group of similar conformations as determined by the values of their dihedral angles. An mc-conformer is a group of conformations with similar backbone dihedral angles. A main chain/side chain (or ms-) conformer is a group of conformations with similar backbone and side chain dihedral angles. The nomenclature for β-turns in the study by Richardson [19] is used to name the mc-conformers. In this study, the word 'bend' following the turn type does not imply H-bonds between residues immediately adjacent to the turn residues.

The main purpose of the present study is to compute and characterize the lowest energy conformations of CVIM in an aqueous environment. The computed conformations give us a better understanding of the binding with FTase. A relationship between the important conformations is proposed. The information obtained here should be useful in the design of experiments to determine pharmacophoric properties. Based on the limited number of computed low energy conformational states and the size of CVIM, the peptide is a good test case for studies of physical properties (such as solvation and electrostatics). The knowledge and expertise obtained in this study should be useful in the conformational analysis of other peptides.

Methodology

Coordinates and energy function

In both the MCSA conformational search and MMC simulations, the peptide geometry was generated by the ECEPP/2 protocol [20], in which bond lengths and bond angles are held fixed and dihedral angles may vary. L-Amino acids were employed. The peptide conformations were computed in an aqueous environment, i.e. the peptide with ionized N- and C-termini, solvation based on solvent accessible surface area and

a distance dependent dielectric of 4r. Explicit water molecules were not considered. Preliminary calculations explored the use of various values for the dielectric constant.

Total energy, F, is the sum of the peptide conformational energy, E, and the solvation free energy, J, and is given by

$$F = E + J \tag{1}$$

Conformational energy is the sum of Lennard-Jones non-bonded, electrostatic and torsion potentials [20]. CHARMm parm20 all atom energy parameters [21] were employed. Hydrogen bond energy is built into the electrostatic charges centered on the nuclei.

Solvation free energy is given by

$$J = \sum_i A_i \sigma_i \tag{2}$$

where A_i is the solvent accessible surface area of atom i and σ_i is the atom solvation parameter. Solvation parameters used were the SRFOPT parameter set [22] and the parameters for charged atoms reported in Reference 23. Solvent accessible surface areas of heavy atoms were computed using MSEED [24] with a 1.4 Å probe radius.

The ECEPP geometric parameters should be transferable between parameter sets since they are based on the equilibrium X-ray conformations of proteins. The solvation parameters should be transferable because they were obtained from small molecule data.

MCSA and MMC protocols

MCSA conformational searches and MMC simulations used the program Salp/2, which is an enhanced version of the program that was used in Reference 14. Conformational searches consisted of multiple independent MCSA runs. The final conformation of each MCSA run was the starting point for an MMC run. The enhanced MCSA methodology is described next, followed by a summary of program enhancements, and a description of the MMC methodology.

An MCSA calculation looped through 300 independent conformational search runs, each starting from a random conformation. In the assignment of dihedral angle values to the 300 random starting conformations, side chain χ angles were randomly assigned from a rotamer library backbone ω angles were set to 180°; and backbone ϕ and ψ angles were randomly assigned in the range $\pm$180° by the use of a random number generator. The nomenclature of dihedral angles is in accordance with Reference 17.

Each MCSA run consisted of 'equilibration' followed by 'prediction'. Separate Boltzmann temperature factors, RT (in kcal/mol), were used to evaluate main chain and side chain trial conformations, in order to make the transition between random and folded states occur at about the same place in the annealing. An MCSA run started out with high Boltzmann temperature factors. As the Boltzmann temperature factors are lowered during an MCSA run, the conformational search is restricted to lower energy pathways. MCSA protocol parameters are summarized in Table 1.

An MCSA run consisted of a specified number of annealing steps. In an annealing step, a specified number of trial conformations (NCON) were sequentially evaluated. NCON was specified for the first equilibration step, the remaining equilibration steps, and the prediction steps.

In trial conformation generation, one of ϕ, ψ, ω or χ was randomly selected; and a new value was randomly assigned in the range $\pm$PERT° of the current value. PERT is the perturbation. Certain dihedral angles were varied in pairs. Selection of ϕ (or ψ) of residue i resulted in trial values for both ϕ_i and ψ_{i-1} (or ψ_i and ϕ_{i+1}). Selection of χ_1 or χ_2 resulted in trial values for both.

An MCSA cycle is defined as the process of evaluating a trial conformation. First, a trial conformation is generated; and the total energy computed. The energy of the trial conformation is compared to the energy of the previously accepted conformation. Trial conformations are accepted or rejected by the use of the Metropolis criteria [25]. The most recently accepted trial conformation is used in the next cycle.

Except for the first and last steps of an MCSA run, the Boltzmann temperature factors were reduced at the end of each MCSA cycle. In the first step, a constant temperature helps remove steric interactions present in the random starting conformation. In the last step, the peptide conformation is optimized at the low temperature. Lowering Boltzmann temperature factors at the end of an MCSA cycle allows slow annealing in the region where the peptide folds. The simulated annealing consisted of two sequential periods of exponential cooling. Boltzmann temperature factors were specified for the first and last equilibration step, RTeqi and RTeqf, and the last prediction step, RTprf. Plots of RT versus number of trial conformations gave plateaus as RT approached RTeqf and RTprf. The current Boltzmann temperature factors were reduced through division by a parameter called β

Table 1. Protocol used in MCSA and MMC runs

Parameter[a]	MCSA		MMC	
	Equilibration[b]	Prediction[c]	Equilibration[b]	Production[c]
NSTEP	11	14	1	1
NCON	1500 (3000 in step 1)	1500	15 000	25 000
RT main chain	8.0 to 4.0	4.0 to 0.6	0.6	0.6
RT side chain	4.0 to 2.0	2.0 to 0.6	0.6	0.6
NPRCHK	2 (5 in step 1)	2	6	10
Parameter[a]	MCSA		MMC	
PERT	±180° backbone, ±180° side chain		±10° backbone, ±30° side chain	
XACRAT	35% main chain trial conformations 40% side chain trial conformations		40% main chain trial conformations 40% side chain trial conformations	
PERTRD	1.7 for both main chain and side chain perturbations		1.5 for both main chain and side chain	

[a]NSTEP is the number of steps. NCON is the number of trial conformations evaluated in the step. RT is the Boltzmann temperature factor in kcal/mol. NPRCHK is the number of times the acceptance ratio is checked in each step. PERT are the initial perturbations used to generate trial conformations. XACRAT is the acceptance ratio limit. PERTRD is the factor used to lower the perturbation.
[b]Parameters for equilibration.
[c]Parameters of MCSA prediction or MMC production.

defined for both main chain and side chain RT. The values of β used during equilibration and prediction, βeq and βpr, respectively, are given by

$$\beta eq = \{RTeqi/RTeqf\}\hat{}(1/(NCONeq\ (NSTEPeq - 1) - 1)$$

and

$$\beta r = \{RTeqf/RTprf\}\hat{}(1/(NCONpr\ (NSTEPpr - 1)) \quad (3)$$

The fraction of trial conformations accepted (called the acceptance ratio) was determined after a specified number of trial conformations were evaluated. If the acceptance ratio fell below the acceptance ratio limit, the perturbation was reduced by a factor of 1.7. If the acceptance ratio rose above the acceptance ratio limit plus 10%, the perturbation was increased by a factor of 1.1. Increasing the perturbation helps the conformational search avoid the local minimum problem.

Enhancements to the MCSA conformational search/MMC program were made in the assignment of NCON, the annealing schedule, the evaluation of acceptance ratios, and the adjustment of perturbations. All changes reduced the computational effort needed to compute the native X-ray conformations of protein surface loops starting from random conformations (manuscript in preparation).

Conformational search options used to generate trial conformations were: (a) the use of a dihedral angle rotamer library, and (b) altering the rate at which main chain and side chain dihedral angles are selected. These options were tested in Reference 26, and later implemented with little refinement in Reference 14. In the χ-rotamer option, a rotamer library was used to generate side chain trial conformations. In the ω-rotamer option, trans to cis transitions occurred with a 10% probability; and cis to trans transitions were always allowed. In the φ/ψ-rotamer option, φ/ψ-rotamer values were chosen 10% of the time when either φ or ψ was selected. In the selection rate option, the probability that a main chain trial conformation was evaluated was increased 20% from 0.58 to 0.70; and the probability that a side chain trial conformation was evaluated was decreased from 0.42 to 0.29. The φ/ψ-rotamer option was turned on for main chain RT between 8.0 and 7.5 kcal/mol (steps 1 and 2). The χ-rotamer option, the ω-rotamer option and the selection rate option were turned on in steps 1 to 11, i.e. for side chain RT between 4.0 and 2.0 kcal/mol and for main chain RT between 8.0 and 4.0 kcal/mol. The value of ω was held fixed for RT between 4.0 and 0.7 kcal/mol (steps 12 to 23); it was freely varied below RT = 0.7 kcal/mol (steps 24 and 25). The values

of the parameters were determined by trial and error [26].

The conformation at the end of each MCSA conformational search run was the starting point for a single molecule MMC run at room temperature, RT = 0.6 kcal/mol. MMC protocol parameters are given in the right-hand side of Table 1. The option to vary dihedral angles in pairs was employed. The rotamer options and the selection rate option were not used. Dihedral angles of the current accepted conformation were saved at intervals of 200 trial conformations during the MMC production step.

Conformational analysis

An enhanced conformational analysis program (called Popen/2) was used to separate and characterize peptide conformers. In the separation process, each residue of each conformation was assigned an alphabetic tag (called a rotamer tag) that specified the conformation of the ϕ/ψ pair, ω, and each χ. A main chain (mc-) rotamer tag consisted of a ϕ/ψ-rotamer tag (in upper case), and an ω-rotamer tag (in lower case or special characters). The general ϕ/ψ-rotamer regions and corresponding ϕ/ψ-rotamer tags are depicted in Figure 1. Mc-rotamer regions and mc-rotamer tags used to separate conformers were defined by the user for each residue of each conformer. For CVIM, three rotamers defined the conformations of side chain dihedral angles, namely, $-60\pm60°$, $180\pm60°$ and $60\pm60°$. Let us call a group of conformations with the same sequence of mc-rotamer tags an mc-conformer and a group of conformations with the same sequence of main chain and side chain rotamer tags an ms-conformer.

In the general separation process, a cluster of residue conformations visualized in ϕ/ψ- and ψ/ω-scatter plots was selected by specifying the rotamer regions, which consisted of upper and lower values of ϕ, ψ and ω. In the separation of an mc-conformer of CVIM, four sets of ϕ, ψ and ω rotamers, one set for each residue, were needed. The separation process required a significant amount of human interaction.

In the interactive separation of mc-conformers, scatter plots that contained all conformations that were within 5 kcal/mol of the lowest energy conformation (LEC) plotted were generated. Next, rotamer regions for each separable cluster of each residue were defined. Conformations that did not belong to one of the separated conformers were plotted; and the separation process was continued. The separation process involved repeated adjustment of rotamer regions for each conformer until the conformers were cleanly separated.

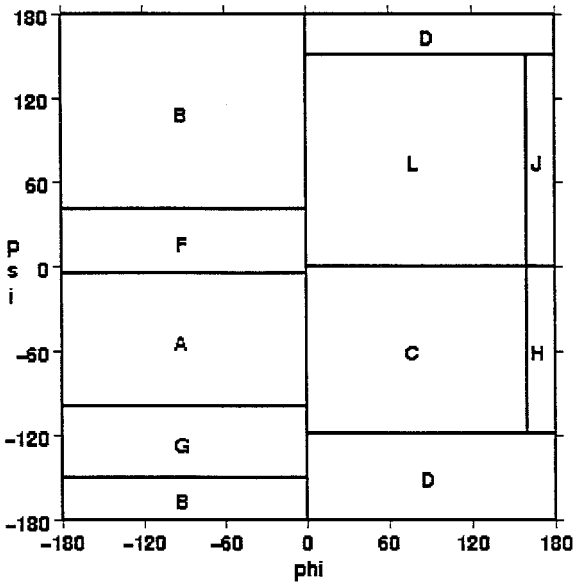

Figure 1. Ramachandran plot of main chain ϕ/ψ-rotamer regions used to identify main chain conformations of each residue of the peptide.

A group of similar conformations that made up a conformer were within 5 kcal/mol of each other. The analysis of all conformations, which would have included conformations that were significantly high in energy, was beyond the scope of the present study; and it would have put a great demand on the parameter set employed.

Two mc-conformers are cleanly separated if there are two separable clusters of ϕ, ψ, or ω conformations of a single residue. The clusters of remaining ϕ, ψ and ω conformations can overlap. Two separable clusters of conformations occur when the energy barrier between the clusters is greater than the energy cutoff. Otherwise, the residue rotamer region boundary must cross near the saddle point on the potential energy surface between clusters.

Conformers that significantly overlapped were not separated. For clusters that did not significantly overlap, the energy cutoff used to select conformations was varied to locate saddle point regions. Here, improper placement of the rotamer region boundary could give rise to errors in the Boltzmann average properties. Conformers that significantly overlap can be separated by decreasing the energy cutoff for conformations plotted, and adjusting the size of a residue rotamer region so that only the low energy region of one of

the overlapping clusters is selected. An option not currently possible is the use of rotamer regions in the form of a circle or ellipse.

Boltzmann average properties of conformer k are computed using the partition function of conformer k given by

$$Q_k = \sum_i \exp(-F_i/RT). \quad (4)$$

where F_i is the total energy of conformation i in conformer k, R is the gas constant, 1.987 cal K^{-1} mol^{-1}, and T is the temperature in Kelvin. For conformer k, the entropy, S, is

$$S_k = R \ln Q_k + 1/(T Q_k) \sum_i F_i \exp(-F_i/RT) \quad (5)$$

The magnitude of conformer entropy gives an indication of the density of conformations that have energies close to the energy of the conformer LEC. Boltzmann average properties computed are average total energy and average conformation of ms-conformers. The Boltzmann average property, $\overline{W}_k$, is given by

$$\overline{W}_k = 1/Q_k \sum_i W_i \exp(-F_i/RT) \quad (6)$$

where W_i is the property of a conformation in conformer k.

Results

Convergence of MCSA conformational searches

Proof that the MCSA conformational search converged was the absence of new separable low energy conformers on additional conformational searches. Two factors ensured that the conformational searches were not forced down the same path. The ϕ/ψ-scatter plots of conformations obtained at high RT showed that the simulations thoroughly explored conformational space. In addition, a new random conformation was generated for the start of each MCSA conformational search run. The results of a conformational analysis on the 300 MCSA final conformations of CVIM are given in Table 2. Columns 1 to 3 are mc-conformer number, relative total energy, and population, respectively. Conformers were ordered by increasing total energy. Columns 4 to 7 are the mc-rotamer tags for each amino acid starting from the N-terminus. Due to space, just the 10 lowest energy mc-conformers are reported.

Table 2. Convergence of CVIM MCSA conformational search[a]

Mer #[b]	$\overline{F}$[c]	Ncon[d]	mc-rotamer tags[e]			
			Cys	Val	Ile	Met
1	0.0	80	B	B	B	B
2	1.8	52	B	B	A	B
3	1.9	31	B	A	B	B
4	2.2	13	B	A	A	B
5	2.3	1	B+	A	B	B
6	2.6	2	B	A+	B	B
7	3.2	1	A	B+	B	B
8	3.4	1	B	B	A−	B
9	3.6	9	A	B	B	B
10	3.7	2	B	A	B+	B

[a] Characterization of a truncated set of 10 lowest total energy mc-conformers obtained from the final conformations of the 300 MCSA conformational searches.
[b] Conformer number ordered by increasing total energy.
[c] Relative Boltzmann averaged total energy in kcal/mol (see Equations 1 and 6).
[d] Conformer population in terms of number of MCSA final conformations.
[e] Mc-rotamer tags of residues listed from N- to C-terminus in the second row are given. ϕ/ψ-rotamer tags correspond to the general regions depicted in Figure 1. Omega rotamer tags which are appended to ϕ/ψ-rotamer tags are '': trans, '+': distorted in 90° direction, and '−': distorted in −90° direction.

The lowest energy mc-conformers were significantly populated. According to Table 2, 80 independent MCSA runs out of 300 converged on the extended conformer (conformer 1), 52 led to the BA-bend conformer (conformer 2), 31 led to the AB-bend conformer (conformer 3), and 13 led to the Type I bend conformer (conformer 4). Prefixes 'BA' and 'AB' specify the conformations of Val 2 and Ile 3. 'B' is for β-strand; 'A' is for α-helix.

Interactive separation of conformers

The ϕ/ψ-scatter plots illustrated in Figure 2 show the CVIM mc-conformers obtained in the MMC calculation. All conformations that have energies within 5 kcal/mol of the LEC are plotted. Due to symmetry at the ionized N- and C-termini, the conformations of Cys ϕ (top plot) were adjusted to lie in the range −120° to 0°; and the conformations of Met ψ (bottom plot) were adjusted to lie in the range 0° to 180°. Val and Ile each had two populated states which gave rise to four possible conformers, namely, the Type I bend, extended, AB-bend, and BA-bend. In these conformers, Cys and Met populated the β-strand region. The

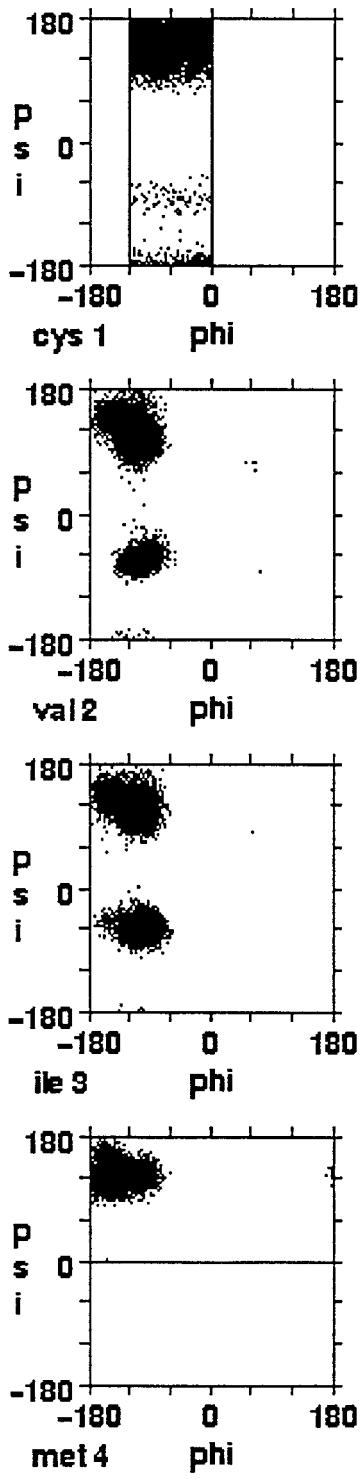

Figure 2. ϕ/ψ-scatter plots of CVIM conformations before interactive separation of conformers. Conformations plotted have energies that are within 5 kcal/mol of the energy of the LEC.

ϕ/ψ conformations of Val and Ile populated either the α-helix region and/or the β-strand region. The absence of conformations in the saddle point region that connects the mc-conformers allowed a clean separation of states.

The structures and thermodynamic properties computed for mc-conformers of CVIM are shown in Table 3. Columns 1 to 3 are the conformer number, the relative average total energy, and entropy, respectively. Conformers were ordered by increasing total energy. Columns 4 and 5 are the number of conformations and fraction population, respectively. Columns 6 to 9 are mc-rotamer tags for each residue starting from the N-terminus. The last column defines the structural motif.

The four lowest total energy CVIM conformers were a Type I bend, extended, AB-bend, and BA-bend (conformers 1 to 4 in Table 3). The average total energies of these conformers were within 0.3 kcal/mol of each other. The entropies of the extended and Type I bend conformers, 13.4 cal K^{-1} mol^{-1} and 9.5 cal K^{-1} mol^{-1}, respectively, indicated a greater density of conformations near the LEC of the extended conformer.

Conformations of residues of conformer 6 are assigned a 'Zz' mc-rotamer tag. These conformations are scattered over the Ramachandran plot. They are conformations that remain after the clusters of conformations given in the table have been separated.

Side chain conformational analysis

Side chain rotamer fraction populations of the four lowest energy conformers of CVIM are reported in Table 4. The χ-rotamer definitions are given in column 1. The fraction populations are reported under the side chain dihedral angles defined across the top row of the table. The number of conformations analyzed for each conformer is given in Table 3. The 180° rotamer of Val χ_1 was always the most populated (Table 4). The conformers had significantly different Ile χ_1 population distributions. The Cys χ_1 population distributions were nearly the same for the extended, AB-bend, and BA-bend conformers. The Met χ_1 population distributions were nearly the same for the Type I bend, AB-bend, and BA-bend conformers. For other side chain angles, the conformers had nearly the same population distributions, namely 0.20, 0.66, and 0.14 for Cys χ_2; 0.05, 0.90, and 0.05 for Met χ_2; and 0.23, 0.57, and 0.21 for Met χ_3.

Table 3. Characterization of CVIM mc-conformers[a]

Mer #[b]	$\overline{F}$[c]	S[d]	Ncon[e]	N_i/N[f]	mc-rotamer tags[g]				Motif[h]
					Cys	Val	Ile	Met	
1	0.0	9.5	895	0.07	B	A	A	B	Type I
2	0.1	13.4	4515	0.35	B	B	B	B	Extended
3	0.1	11.2	1658	0.13	B	A	B	B	AB-bend
4	0.3	12.5	2614	0.21	B	B	A	B	BA-bend
5	1.6	7.6	327	0.03	A	B	B	B	–
6	2.3	6.6	299	0.02	Zz	Zz	Zz	Zz	–
7	2.5	7.9	294	0.02	A	B	A	B	–
8	3.6	5.3	134	0.01	B	B	L	B	–
9	3.7	5.7	95	0.01	B	C	A	B	Type II′
10	3.7	9.4	726	0.06	Bs	L	B	B	–
11	4.4	6.3	147	0.01	Bs	L	A	B	–
12	5.7	5.7	131	0.01	B	B	A	L	–
13	5.8	5.3	138	0.01	B	A	B	L	–
14	6.1	8.9	614	0.05	B	B	B	L	–
15	8.8	6.7	162	0.01	Bs	L	L	B	–

[a]Structures and energies of conformers computed from 37 500 conformations saved during MMC runs. For each conformer, conformations within 5 kcal/mol of the LEC are analyzed.
[b]Conformer number ordered by increasing total energy.
[c]Relative Boltzmann averaged total energy in kcal/mol (see Equations 1 and 6).
[d]Entropy in cal K^{-1} mol^{-1} (see also Equation 5).
[e]Number of conformations in the cluster of conformations that constitute the conformer.
[f]Fraction population relative to total number of conformations of conformers 1 to 15.
[g]Mc-rotamer tags of residues listed from N- to C-terminus in the second row are given. ϕ/ψ-rotamer tags correspond to the general regions depicted in Figure 1. Conformations of ω are trans except for residue 1 of conformers 10, 11 and 15, which have the rotamer tag 's' meaning scattered in a broad range about the trans configuration. Conformations assigned a 'Zz' mc-rotamer tag are conformations that remain after the clusters of conformations given in the table have been separated.
[h]Structural motif based on the sequence of mc-rotamer tags.

Average conformations

Boltzmann average conformations of Type I bend, extended, AB-bend, and BA-bend ms-conformers are given in Table 5. Boltzmann average conformations of the lowest energy ms-conformers are given in terms of the dihedral angles defined in column 1. The number in parentheses next to the average value is the root mean square (rms) deviation from the average. Ms-conformers, ordered by increasing total energy, are given directly underneath the associated mc-conformers defined in the first row. Ms-conformers of an mc-conformer differ in the rotamer conformation of Ile χ_1. An average conformation was determined from the group of conformations that constitute the ms-conformer. A 5 kcal/mol cutoff applied in the selection of the group of conformations. The rms deviation from the average conformation is a measure of the flexibility of the peptide in the conformation. The last three rows of the table give the ms-conformer relative average total energy, average solvation free energy, and number of conformations in the cluster of conformations.

The BA-bend ms-conformer (ms-conformer 1 in Table 5) was the lowest total energy ms-conformer. The lowest energy extended ms-conformer with Cys $\chi_1 = 180°$ (ms-conformer 15) satisfied an important pharmacophoric property, which is discussed below. No hydrogen bonds (H-bonds) were present in the average conformations. H-bond criteria used were a) H-bond length less than 2.5 Å, and (b) H-bond angle, $\angle$(N - H - -O), between 120 and 180°.

Stereoscopic stick diagrams of the average conformations obtained for the lowest energy BA-bend, AB-bend, Type I bend, and extended ms-conformers are depicted in Figures 3a to 3d, respectively. All atoms are represented. The N- and C-termini are la-

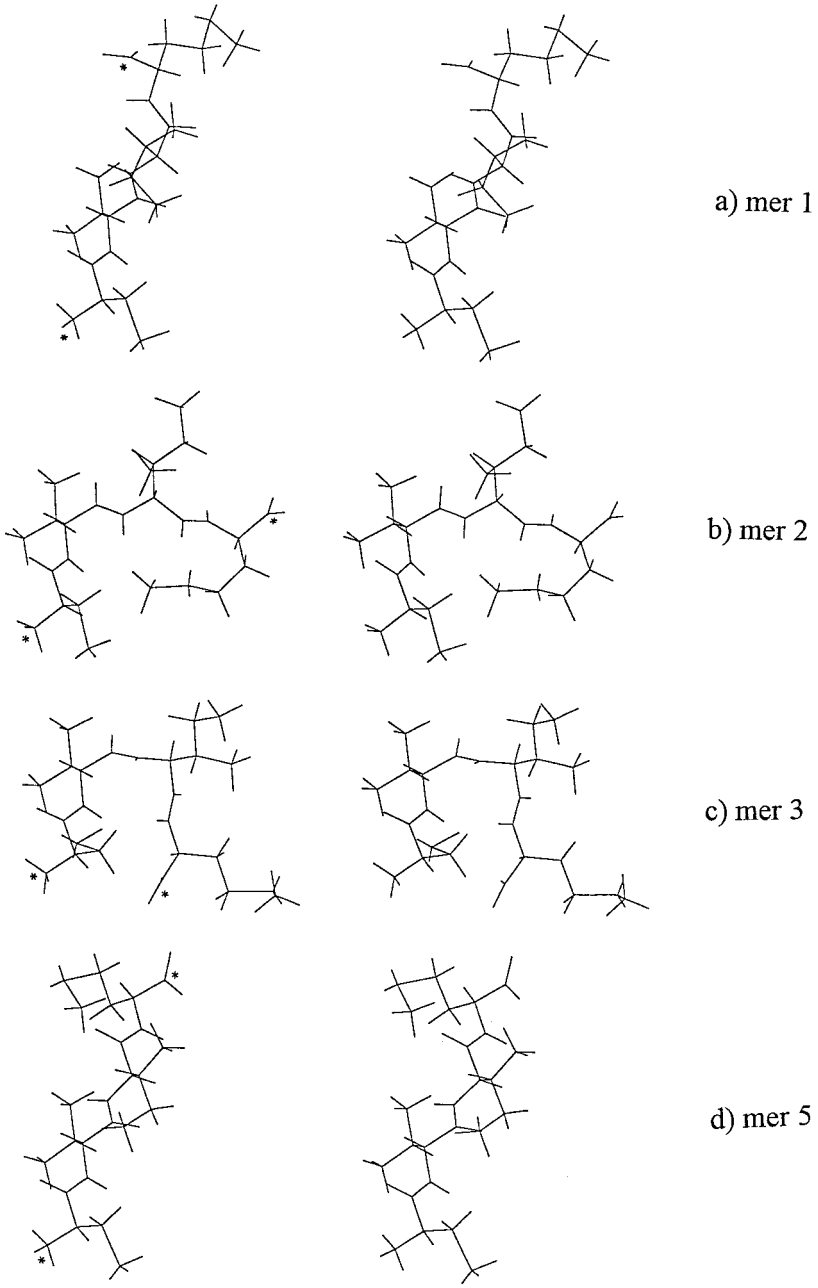

Figure 3. Stereoscopic stick models of average conformations computed for the lowest energy. (a) BA-bend, (b) AB-bend, (c) Type I bend and (d) extended ms-conformers, ms-conformers 1, 2, 3 and 5, respectively. All atoms are plotted. The N- and C-termini are labeled with asterisks. The N-terminus is located at the bottom left.

beled with asterisks. The N-terminus is located at the bottom left.

The average conformations depicted in Figure 3 are shown as superimposed stereoscopic stick models in Figure 4. Only heavy atoms are represented. The BA-bend, AB-bend, and Type I bend conformations were superimposed on the extended conformation. Atoms superimposed were Cys N, C^{α}, C^{β}, C′, and O and atoms Val N, C^{α}, C^{β} and C′. Average overlap deviations and rms errors computed for superimposed atoms of the BA-bend, AB-bend, and Type I bend conformations were 0.08±0.04 Å, 0.22±0.14 Å, and

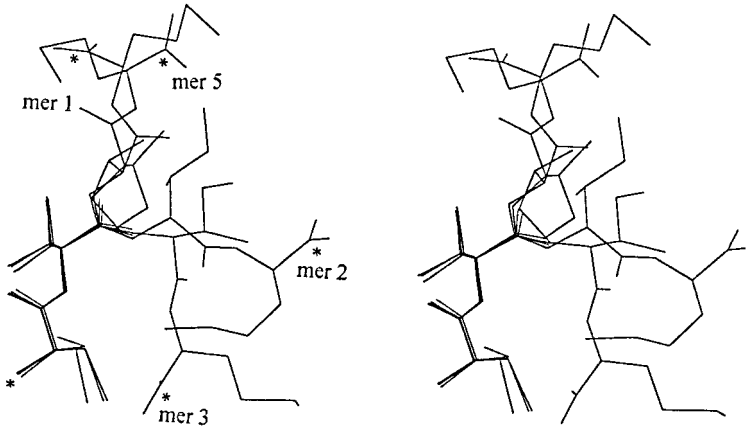

Figure 4. Superimposed stereoscopic stick models of average conformations of BA-bend, AB-bend, Type I bend and extended ms-conformers, labeled mer 1, mer 2, mer 3 and mer 5, respectively. Only heavy atoms are plotted. The N- and C-termini are labeled with asterisks. The N-terminus is located at the bottom left. See text for atoms superimposed.

Table 4. Fraction populations of CVIM χ-rotamers[a]

Rot [b]	Cys χ_1	Val χ_1	Ile		Met χ_1
			χ_1	$\chi_{2,1}$	
Type I bend					
−60	0.45	0.04	0.57	0.07	0.35
180	0.16	0.95	0.25	0.70	0.60
60	0.39	0.01	0.17	0.23	0.05
Extended					
−60	0.78	0.05	0.70	0.06	0.52
180	0.16	0.84	0.26	0.70	0.48
60	0.06	0.11	0.04	0.24	0.00
AB-bend					
−60	0.78	0.02	0.28	0.00	0.35
180	0.13	0.98	0.62	0.83	0.65
60	0.09	0.00	0.10	0.17	0.00
BA-bend					
−60	0.80	0.05	0.87	0.16	0.32
180	0.15	0.78	0.04	0.62	0.61
60	0.05	0.17	0.09	0.22	0.07

[a]Sc-rotamer fraction populations computed for mc-conformers 1 to 4 in Table 3. Residue dihedral angles are given across the first row.
[b]Side chain rotamers. Here, −60, 180, 60 correspond to the −60°±60°, 180°±60°, and 60°±60° rotamers.

0.07±0.03 Å, respectively. The orientations of corresponding conformations in Figures 3 and 4 are the same, the views differ by translation.

The average conformations of the 10 lowest energy extended ms-conformers are superimposed in the stereoscopic stick diagram depicted in Figure 5. The conformations were superimposed on the backbone heavy atoms, N, C^{α}, C^{β}, C′ and O, of residues Val and Ile of the lowest energy conformer average conformation. Average total energies of conformers analyzed spanned 0.6 kcal/mol. The lowest energy conformer average conformation is at the center of the cluster.

Interatomic distances for selected peptide atom pairs in extended, Type I bend, AB-bend, and BA-bend average conformations are given in Table 6. Atom pairs are listed in column 1. Columns 2 to 7 give the interatomic distances. The S^{γ} to C′ distance was larger in the extended ms-conformer 5 conformation compared to the extended ms-conformer 15 conformation due to rotation about Cys χ_1.

Discussion

Comparison with experiment

Based on experimental evidence [11, 13], the extended and Type I bend conformations were the lowest energy conformers computed in an aqueous environment, which was defined as ionized N- and C-termini, continuum solvation model, and a distant dependent dielectric of 4r. The extended and Type I bend conformers were two of the most populated conformers; and they differed in energy by only 0.1 kcal/mol. Two other dominant low energy conformers found were the AB-bend and BA-bend conformers. The extended conformation could be obtained from the AB- and BA-bend conformations by a change in Val ψ and Ile ψ, respectively. The Type I bend conformation could be obtained from the AB- and BA-bend conformations by a change in Ile ψ and Val ψ, respectively. These

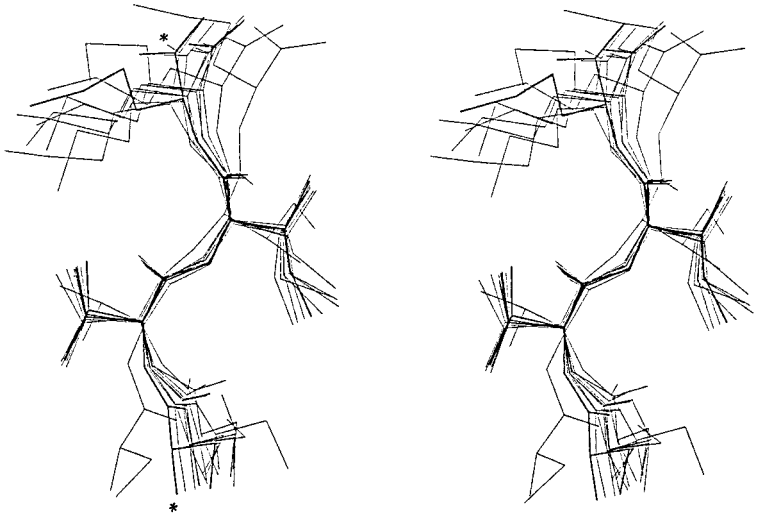

Figure 5. Superimposed stereoscopic stick models of the average conformations of the 10 lowest total energy extended ms-conformers. Only heavy atoms are depicted. The lowest energy conformer average conformation is at the cluster center. N-termini are at the bottom; C-termini are at the top. Both are labeled with asterisks. See text for atoms superimposed.

calculations were not able to predict the influence of peptide/receptor interactions on peptide conformation.

The distance between Cys S^{γ} and the C-terminal carboxyl group in the extended conformation depended in part on the rotamer conformation of Cys χ_1. In the average conformations of mer 5 and mer 15 given in Table 5, the Cys χ_1 rotamers were $-60°$ and 180°, respectively; and the Cys S^{γ} to Met C′ distances were 12.3 and 10.4 Å, respectively. The latter distance is close to the distance between the sulfur atom and the carboxyl carbon in a potent inhibitor of FTase (about 10.5 Å) [11].

Leonard et al. [12] showed that a pentapeptide derivative that lacks cysteine inhibits FTase. The Cys C^{β} to Met C′ distance is a more accurate measure of the length of a conformation since it does not depend on the rotamer conformation of Cys χ_1. The distances between Cys C^{β} to Met C′ in the extended, BA-bend, and AB-bend average conformations were 10.7, 10.3, and 9.1 Å, respectively. In the Type I bend conformation, the Cys C^{β} to Met C′ distance was 4.2 Å. Based on the superposition depicted in Figure 4, the AB-bend conformation is similar in structure to the Type I bend conformation; and the BA-bend conformation is similar in structure to the extended conformation.

Peptide flexibility

Peptide flexibility was demonstrated in the superposition of the backbone of Val and Ile of average extended conformations depicted in Figure 5. Val and Ile superimposed very well. The rms deviations of the Boltzmann average conformations reported in Table 5 characterized peptide flexibility. Large rms deviations are associated with flexibility among the group of conformations of an ms-conformer. Pharmacophoric properties could be developed from peptide mimetics designed to superimpose on the rigid parts of the computed conformations. The side chain conformation population data in Table 4 could be used in the design of a mimetic built up in regions that correspond to the Val and Ile side chains.

Interconversion between conformers

According to the ϕ/ψ-scatter plots depicted in Figure 2, very few conformations along the interconversion paths between the four dominant conformers were observed. Increasing the energy cutoff used to select conformations plotted to 10 kcal/mol did not change the situation. Analysis of trajectories that started from just the extended, Type I bend, AB-bend, and BA-bend conformations indicated that interconversion between the dominant conformers did occur. A quantitative measure of interconversion could not be obtained. This may be due to the fact that the geometric and energy parameters used in the calculations were designed for equilibrium conformations, which the conformations in the transition state region are not. In addition, bond lengths and bond angles were fixed at equilibrium values during the MCSA and MMC runs.

Table 5. Boltzmann averaged conformations of selected ms-conformers[a]

	Type I bend			Extended			AB-bend		BA-bend
	3	23	85	5	15[b]	18	2	11	1
Cys ϕ	**−115 (34)**	**−99 (51)**	**−16 (57)**	**−74 (35)**	**−66 (31)**	**−29 (45)**	**−54 (32)**	**−99 (26)**	**−79 (36)**
ψ	**152 (26)**	**173 (34)**	**141 (21)**	**155 (21)**	**144 (16)**	**150 (24)**	**121 (29)**	**152 (15)**	**145 (20)**
ω	164 (19)	−179 (25)	173 (11)	173 (14)	178 (14)	174 (14)	168 (17)	−154 (21)	168 (16)
χ_1	41 (20)	33 (7)	−67 (27)	−71 (24)	−148 (17)	−77 (25)	−54 (22)	−97 (34)	−65 (22)
χ_2	156 (39)	105 (5)	−132 (48)	−173 (32)	64 (39)	146 (53)	−158 (30)	−72 (22)	−154 (34)
Val ϕ	**−118 (15)**	**−120 (31)**	**−93 (17)**	**−120 (14)**	**−107 (11)**	**−116 (19)**	**−107 (16)**	**−128 (18)**	**−108 (13)**
ψ	**−74 (14)**	**−64 (21)**	**−64 (13)**	**112 (15)**	**88 (20)**	**102 (21)**	**−64 (11)**	**−79 (20)**	**123 (16)**
ω	143 (21)	−172 (11)	−169 (13)	169 (12)	168 (12)	−171 (18)	−174 (10)	170 (4)	−171 (14)
χ_1	180 (8)	179 (6)	176 (7)	180 (11)	−175 (11)	−179 (11)	176 (12)	−178 (8)	−178 (10)
$\chi_{2,1}$	55 (23)	54 (30)	36 (21)	51 (24)	56 (22)	60 (25)	52 (22)	55 (13)	64 (21)
$\chi_{2,2}$	83 (12)	89 (18)	55 (17)	70 (16)	76 (14)	75 (17)	79 (10)	72 (24)	76 (18)
Ile ϕ	**−72 (26)**	**−126 (14)**	**−134 (16)**	**−104 (15)**	**−98 (15)**	**−157 (26)**	**−158 (14)**	**−90 (15)**	**−91 (14)**
ψ	**−60 (10)**	**−66 (15)**	**−63 (13)**	**119 (15)**	**107 (19)**	**139 (13)**	**132 (16)**	**115 (15)**	**−75 (17)**
ω	−164 (13)	−158 (14)	−171 (11)	−177 (14)	174 (10)	176 (13)	171 (12)	175 (18)	−175 (9)
χ_1	−64 (10)	35 (9)	179 (5)	−59 (11)	−56 (15)	−172 (10)	−171 (11)	−55 (10)	−52 (10)
$\chi_{2,1}$	177 (28)	155 (17)	169 (14)	108 (13)	101 (17)	148 (16)	168 (13)	110 (4)	−56 (14)
$\chi_{2,2}$	53 (20)	74 (14)	80 (19)	47 (19)	47 (16)	64 (22)	97 (36)	50 (8)	22 (25)
$\chi_{3,1}$	96 (45)	46 (24)	82 (34)	64 (29)	59 (30)	49 (27)	74 (25)	42 (20)	77 (27)
Met ϕ	**−163 (14)**	**−128 (14)**	**−143 (23)**	**−155 (22)**	**−127 (18)**	**−145 (15)**	**−118 (14)**	**−132 (17)**	**−132 (13)**
ψ	**132 (9)**	**128 (12)**	**141 (19)**	**117 (12)**	**131 (14)**	**114 (12)**	**123 (13)**	**126 (21)**	**127 (11)**
ω	–	–	–	–	–	–	–	–	–
χ_1	178 (18)	−83 (17)	−87 (14)	−175 (19)	−71 (13)	−177 (15)	−64 (14)	−81 (15)	−79 (16)
χ_2	165 (28)	163 (28)	179 (18)	161 (21)	−161 (21)	151 (23)	100 (15)	−159 (14)	175 (25)
χ_3	−109 (27)	−139 (25)	−140 (31)	64 (23)	−142 (37)	60 (31)	−130 (33)	−71 (27)	−147 (45)
χ_4	82 (26)	38 (22)	83 (33)	43 (31)	64 (29)	33 (39)	27 (33)	105 (11)	59 (29)
$\Delta\overline{F}$[c]	0.2	1.0	1.7	0.4	0.8	0.9	0.1	0.7	0.0
$\overline{J}$[d]	−29.8	−33.6	−33.0	−33.2	−33.0	−33.2	−32.5	−33.6	−32.8
Ncon[e]	7	5	12	54	13	66	14	6	29

[a]For each mc-conformer analyzed (conformers 1 to 4 in Table 3), the lowest energy ms-conformer and selected lowest energy ms-conformers that differ in the rotamer conformation of Ile χ_1 are characterized. Mc-conformer numbers and motif types are given in the first row. Mc/sc-conformer numbers ordered by increasing total energy are given in the second row. Column 1 defines the dihedral angle. Numbers in parentheses next to the average values are rms deviations.

[b]Lowest energy ms-conformer with Cys $\chi_1 = 180°$ rotamer.

[c]Relative Boltzmann averaged total energy in kcal/mol (see Equations 1 and 6).

[d]Boltzmann averaged solvation free energy in kcal mol^{-1} (see Equations 2 and 6).

[e]Number of conformations in ms-conformers.

In theory, the extended conformation of the peptide should convert to the classical Type I bend conformation [19] by a change in Val ψ from 90° to −30° and a change in Ile ψ from 90° to 0°. Let us propose a relationship between the four dominant conformers (extended, Type I bend, AB-bend, and BA-bend conformers) that were within 0.3 kcal/mol in total energy. Interconversion between extended and Type I bend conformations could proceed by sequential rotations of Val ψ followed by Ile ψ or vice versa. Another possible mechanism is concerted rotations of Val ψ and Ile ψ. MMC trajectories starting from just one type of conformation (data not given here) gave some support for the sequential mechanism of interconversion.

Separation of conformers

In the MCSA calculation, the extended mc-conformer was the lowest energy conformer by about 1.8 kcal/mol (Table 2). In the MMC calculation, the

Table 6. Select inter-atomic distances in average conformations of ms-conformers[a]

Atom pair[b]	Extended			Type I	AB-bend	BA-bend
	mer 5	mer 15	M10	mer 3	mer 2	mer1
Cys $C^{\beta} \leftrightarrow$ Met C'	10.8	10.6	10.7±0.3	4.2	9.1	10.3
Cys $S^{\gamma} \leftrightarrow$ Met C'	12.3	10.4	11.7±0.9	6.0	9.8	12.0

[a]Inter-atomic distances (Å) between selected atom pairs in average conformations of extended ms-conformers 5 and 15, in average conformations of the 10 lowest energy extended ms-conformers (M10), and in average conformations of Type I bend, AB-bend and BA-bend ms-conformers, ms-conformers 3, 2 and 1.
[b]Peptide atom pairs.

Type I bend mc-conformer was the lowest energy conformer by 0.1 kcal/mol (Table 3). Here, the process of probing the potential energy surface during the MMC calculation led to a low energy Type I bend conformation. In the MMC calculation, the lowest energy mc-conformer had a different main chain conformation compared to the lowest energy ms-conformer. The BA-bend ms-conformer was the lowest energy ms-conformer by 0.1 kcal/mol (Table 6). Boltzmann averages affected the relative total energies of the conformers by a few tenths of a kcal/mol.

Due to significant overlap in the scatter plots of the extended mc-conformer, clusters in the β-strand regions of Val and Ile were not separated. For the same reason, distorted and trans conformations of Val ω in the Type I bend mc-conformer were not separated. In this case, the separation was made possible by clustering conformations in terms of ms-conformers. The range of Val ω in ms-conformer 3 in Table 5, 143°±21°, was significantly outside the range observed in ms-conformers 23 and 85, −172°±11° and −169°±13°, respectively.

Solvation free energy

The average solvation free energies of ms-conformers reported in Table 5 ranged from −30 to −34 kcal/mol. According to Makhatadze and Privalov [27], the entropies due to hydration of polar and non-polar groups are both negative due to an increase in structured water. The negative solvation free energies computed in the present study are due to the negative enthalpy of hydration. The non-covalent interaction energy between water and peptide significantly outweighs the positive entropy contribution to hydration free energy, $-T\Delta S_{hyd}$, interpreted by Makhatadze and Privalov.

Parameter sets and explicit water

Changing the dielectric constant to 2r from 4r influenced the order of the conformers in terms of relative total energy but did not significantly influence the populations of the conformers. In the CVIM calculation computed with a dielectric of 2r (data not tabulated here), the relative total energies of the extended, AB-bend, and BA-bend conformers were 4.6 kcal/mol above the energy of the Type I bend conformer. Low energy Type I bend conformers that had ω dihedral angles distorted in the +90° direction were observed. Also, a low energy Type II′ bend conformer was observed.

The dominant conformers of CVIM computed with ionized end groups and with a vacuum dielectric ($\varepsilon = 1$; data not given here) corresponded to a low energy Type I bend and a high energy Type II′ bend. The extended conformer appeared as a significantly populated high energy conformer when the peptide was studied with neutral end groups and $\varepsilon = 1$. The use of implicit solvation in the calculation with neutral end groups made the relative total energy of the extended conformer zero. These results are consistent with those of the Met-Enk study [14].

Two issues recently investigated by Rick and Bern, the use of an implicit solvation model in place of explicit water [28], and the use of fixed point charges on atoms [29], may have influenced the results of this study. Explicit water could be important when there are one or more water molecules that form multiple hydrogen bonds with the peptide (or structured water molecules). In a comparison of a continuum model versus molecular dynamics [28], significant errors in the solvation free energies were attributed mostly to the dependence of atomic radii on charge. The cost of the use of explicit water is a much less robust conformational search for the same amount of time. In another study, the use of a dynamically fluctuat-

ing charge (FQ) force field better reproduced physical properties of solutes [29]. Based on the size of the CVIM peptide and the small number of CVIM conformers found in the present study, CVIM should be used as a test case to better understand the solvation effects described above.

Conclusions

Conformational states of CVIM in an aqueous environment were successfully computed using the MCSA/MMC approach. The four lowest energy conformers, which were within 0.3 kcal/mol of each other and dominant in terms of population, were consistent with the experimental observations. The AB-bend conformation was similar in structure to the Type I bend conformation; and it had an end-to-end distance comparable to the extended conformation. The BA-bend conformation was very similar to the extended conformation. The Cys C^{β} to Met C' distance was a good measure of peptide length. A mechanism of interconversion between extended and Type I bend conformations could involve the AB-bend and BA-bend conformations as intermediates. The results of this study should be useful in the design of experiments to develop pharmacophoric properties. Compared to the previous version of Popen, the separation of conformers using the revised program Popen/2 was more accurate and the average properties were more reliable. The knowledge and experience obtained in this study should be useful in the conformational analysis of other peptides and protein surface loops, and in the analysis of physical properties of small molecules.

Acknowledgements

Careful reading of the manuscript and helpful discussions with Dr. Arthur Edison are gratefully acknowledged. Computing resources for the MCSA conformational search and MMC calculations were in part generously provided by Academic Computing at USF. Reviewer comments are greatly appreciated.

References

1. Grand, B.A. and Owen, D., Biochem. J., 279 (1991) 609.
2. Barbacid, M., Annu. Rev. Biochem., 56 (1987) 779.
3. Der, C.J. and Cox, A.D., Cancer Cells, 3 (1991) 331.
4. Hancock, J.F., Magee, J.E. and Marshall, C.J., Cell, 57 (1989) 1167.
5. Casey, P.J., Solski, P.A., Der, C.J. and Buss, J.E., Proc. Natl. Acad. Sci. USA, 86 (1989) 8323.
6. Gutierrez, L., Magee, A.I., Marshall, C.J. and Hancock, J.F., EMBO J., 8 (1989) 1093.
7. Reiss, Y., Seabra, M.C., Goldstein, J.L. and Brown, M.S., Methods, 1 (1990) 241.
8. Reiss, Y., Goldstein, J.L., Seabra, M.C., Casey, P.J. and Brown, M.S., Cell, 62 (1990) 81.
9. Leonard, D.M., J. Med. Chem., 40 (1997) 29721.
10. Qian, Y., Blaskovich, M.A., Saleem, M., Seong, C.M., Wathen, S.P., Hamilton, A.D. and Sebti, S.M., J. Biol. Chem., 269 (1994) 12410.
11. Qian, Y., Vogt, A., Sebti, S.M. and Hamilton, A.D., J. Med. Chem., 39 (1996) 217.
12. Leonard, D.M., Shuler, K.R., Poulter, C.J., Eaton, S.R., Sawyer, T.M., Hodges, J.C., Su, T., Scholten, J.D., Gowan, R.C., Sebolt-Leopold, J.S. and Doherty, A.M., J. Med. Chem., 39 (1996) 217.
13. Stradley, S.J., Rizo, J. and Gierasch, L., Biochemistry, 32 (1993) 12586.
14. Carlacci, L., J. Comput.-Aided Mol. Design, 12 (1998) 195.
15. McKelvey, D.R., Brooks, C.L. and Mokotoff, M., J. Protein Chem., 10 (1991) 265.
16. Zimmerman, S.S., Pottle, M.S., Némethy, G. and Scheraga, H.A., Macromolecules, 10 (1977) 1.
17. IUPAC-IUB Commission on Biochemical Nomenclature, Biochemistry, 9 (1970) 3471.
18. Karpen, M.E., Tobias, D.J. and Brooks, C.L., Biochemistry, 32 (1993) 412.
19. Richardson, J.S., Adv. Protein Chem., 34 (1981) 167.
20. Némethy, G., Pottle, M.S. and Scheraga, H.A., J. Phys. Chem., 87 (1983) 1883.
21. CHARMm is a trademark of Molecular Simulations Inc., San Diego, CA.
22. Vila, J., Williams, R.L., Vasquez, M. and Scheraga, H.A., Proteins Struct. Funct. Genet., 10 (1991) 199.
23. Wesson, L. and Eisenberg, D., Protein Sci., 1 (1992) 227.
24. Perrot, G., Cheng, B., Gibson, K.D., Vila, J., Palmer, K.A., Nayeem, A., Maigret, B. and Scheraga, H.A., J. Comput. Chem., 13 (1992) 1.
25. Metropolis, N., Rosenbluth, A.W., Rosenbluth, M.N., Teller, A.H. and Teller, E.J., Chem. Phys., 21 (1953) 1087.
26. Carlacci, L. and Englander, S.W., J. Comput. Chem., 17 (1996) 1002.
27. Makhatadze, G.I. and Privalov, P.L., Protein Sci., 5 (1996) 507.
28. Rick, S.W. and Berne, B.J., J. Am. Chem. Soc., 116 (1994) 3949.
29. Rick, S.W. and Berne, B.J., J. Am. Chem. Soc., 118 (1996) 672.